*Article*

# Species of the *Colletotrichum* spp., the Causal Agents of Leaf Spot on European Hornbeam (*Carpinus betulus*)

Yu-Hang Qiao [1,2,†] , Chen-Ning Zhang [1,2,†], Min Li [1,2] , Huan Li [1,2], Yun-Fei Mao [3] and Feng-Mao Chen [1,2,*]

1 College of Forestry, Nanjing Forestry University, Nanjing 210037, China
2 Collaborative Innovation Center of Sustainable Forestry in Southern China, Nanjing 210037, China
3 Suzhou Forestry Station, Suzhou 215100, China
* Correspondence: cfengmao@njfu.edu.cn
† These authors contributed equally to this work.

**Abstract:** European hornbeam (*Carpinus betulus* L.) is widely planted in landscaping. In October 2021 and August 2022, leaf spot was observed on *C. betulus* in Xuzhou, Jiangsu Province, China. To identify the causal agent of anthracnose disease on *C. betulus*, 23 isolates were obtained from the symptomatic leaves. Based on ITS sequences and colony morphology, these isolates were divided into four *Colletotrichum* groups. Koch's postulates of four *Colletotrichum* species showed similar symptoms observed in the field. Combining the morphological characteristics and multi-gene phylogenetic analysis of the concatenated sequences of the internal transcribed spacer (ITS) gene, Apn2-Mat1-2 intergenic spacer (ApMat) gene, the calmodulin (CAL) gene, glyceraldehyde3-phosphate dehydrogenase (GAPDH) gene, Glutamine synthetase (GS) gene, and beta-tubulin 2 (TUB2) genes, the four *Colletotrichum* groups were identified as *C. gloeosporioides*, *C. fructicola*, *C. aenigma*, and *C. siamense*. This study is the first report of four *Colletotrichum* species causing leaf spot on European hornbeam in China, and it provides clear pathogen information for the further evaluation of the disease control strategies.

**Keywords:** *Carpinus betulus*; *Colletotrichum*; leaf spot; identification

## 1. Introduction

European hornbeam (*Carpinus betulus* Linnaeus) belongs to the family Betulaceae and is mainly distributed in temperate and subtropical regions. It is native to peripheral forests around Europe, Asia Minor, and the Caspian Sea, and is often mixed with oak and beech. It can grow well above 1000 m above sea level [1]. In Iran, European hornbeam is the main tree species in the wood industry, with excellent technical performance and great application potential. It is mainly used for manufacturing tool handles, furniture, and paper, and it is also an excellent wood for railway sleeper production and dam reinforcement after preservative treatment [2]. European hornbeam is also very popular in urban green spaces and parks, and it has excellent characteristics of cold resistance, drought resistance, and pruning resistance. European hornbeam has been selected as an important tree species in garden construction since the Italian Renaissance [3]. In addition, it has been reported that many anticancer substances can be extracted from the young stems and leaves of European hornbeam, such as pheophorbide A (PHA) and some triterpenoids [4,5]. Therefore, European hornbeam has great research value and practical potential.

The genus *Colletotrichum* Corda is the only genus of Glomerellaceae [6] and one of the ten most important plant pathogenic fungi in the world [7]. The fungi of the genus *Colletotrichum* are distributed worldwide, with diverse host plants, including more than 3000 species of monocot and dicot plants [8,9]. Some *Colletotrichum* species can also cause human infection and inflammation, such as *Colletotrichum gloeosporioides* [10,11].

Before the 1990s, the classification of *Colletotrichum* was mainly based on morphological characteristics. The morphological classification of the genus *Colletotrichum* is mainly

based on the morphology and size of conidia, the appressorium, the sporulation structure and conidiophores, and the presence and morphology of chlamydospores, setae, and sclerotia [12–14]. However, because of the instability of these characteristics, the classification of *Colletotrichum* is very confusing [12,15,16]. With the rapid development of molecular biology, the method based on morphology combined with molecular biological identification has gradually been used for the classification of *Colletotrichum* and has been widely used [17,18]. The internal transcribed spacer (ITS) is easy to analyze; however, the sequence of ITS fragments within species is relatively consistent. Therefore, it is difficult to accurately identify a species by its ITS fragments [19]. Multi-gene sequence analysis is increasingly applied to the classification of *Colletotrichum*, and the frequently used gene loci include the calmodulin (CAL) gene, glyceraldehyde3-phosphate dehydrogenase (GAPDH) gene, beta-tubulin 2 (TUB2) gene, chitin synthase (CHS-1) gene, actin (ACT) gene, Glutamine synthetase (GS) gene, Apn2-Mat1-2 intergenic spacer (ApMat) gene, etc.

*Colletotrichum fructicola*, *C. aenigma*, *C. gloeosporioides*, and *C. siamense* all belong to the *Colletotrichum gloeosporioides* species complex. These four species are more or less typical of the generalized *C. gloeosporioides* reported in the past half century in terms of morphology [20]. *C. fructicola* was first reported on *Coffea* in Thailand, and its hosts are diverse in terms of biology and geography, including *Coffea*, *Dalbergia hupeana*, and *Millettia speciosa* in different countries [21–23]. *C. aenigma* was named based on its mysterious biological and geographical distribution. It was first discovered in Italy and Japan, and consistent with the prediction of Weir et al., it has been gradually reported in China, Thailand, and South Korea in recent years [24–26]. *C. gloeosporioides* is common worldwide and easily found on *Citrus*, but it also infects other hosts, including papaya and *Rubia cordifolia* [27–29]. *C. siamense* was also first reported on *Coffea* in Thailand, and its hosts also exhibit diversity in biology and geography, such as *Plukenetia volubilis* in China, *Annona muricata* in Brazil, and *Capsicum annuum* in the Andaman and Nicobar Islands [30–32].

At present, the diseases reported for European hornbeams mainly include the powdery mildew of leaves, the canker of branches, and root rot. The pathogens of powdery mildew vary among areas. Piątek reported that *Oidium carpini* caused powdery mildew in Poland [33], Vajna reported that the pathogen of powdery mildew in Hungary was *Erysiphe carpinicola* [34], and Pastircakova found that the new pathogen of powdery mildew in Slovakia was *Erysiphe arcuata*, which Chinan also reported in Romania [35,36]. There are few reports of canker and root rot. Rocchi reported that branch cankers in Italy were caused by *Anthostoma decipiens* [3]. Mao reported that *Fusarium oxysporum* caused root rot in Jiangsu Province, China [37]. Recently, in Xuzhou, Jiangsu Province, China, European hornbeam was found to have symptoms of leaf spots, which affected the local landscape and economic development in this area.

This study aims to identify the pathogenic fungi that cause leaf spot disease from the aspects of phylogeny and morphology and to study their biological characteristics and pathogenicity, ultimately to provide a theoretical basis for the prevention and control of leaf spot disease in European hornbeam.

## 2. Materials and Methods

### 2.1. Sampling and Fungal Isolation

The field survey was investigated in Xuzhou Urban Garden Company (34.28° N, 118.03° E) in October 2021 and August 2022 in Xuzhou, Jiangsu Province. Xuzhou has a temperate monsoon climate with four distinct seasons, the annual sunshine hours are 2284–2495 h, the sunshine rate is 52–57%, the average annual precipitation is 800–930 mm, and the rainy season precipitation accounts for 56% of the whole year.

Diseased leaves were collected from a 1–2 m part of European hornbeam. Approximately 30 diseased samples were collected from 10 European hornbeam trees which were scattered in the field. Fungi isolation was conducted on the second day after field survey. The diseased leaves were disinfected in 1% sodium hypochlorite for 90 s, rinsed in sterile water twice for 30 s, and dried with sterile paper. Then, the tissues from the margin of

the lesions (0.2 cm × 0.2 cm) were excised, incubated on 2% potato dextrose agar (PDA) supplemented with 100 mg/L ampicillin sodium, and incubated in the dark at 25 °C for 4 days. Fungal hyphae grown from the leaf tissues were picked up and transferred to fresh PDA within 2–4 days [38].

### 2.2. Pathogenicity Tests

Healthy European hornbeam saplings with a height of approximately 1 m were obtained from Xuancheng Garden Greening Co., Ltd. in Xuancheng, Anhui Province.

Before the pathogenicity experiment, the surfaces of the leaves were sprayed with 75% alcohol 2–3 times, and then the above operation was repeated with sterile water to remove the residual alcohol; then, they were dried with absorbent paper, or we waited for the surfaces to dry. The spore suspension ($10^6$ conidia·mL$^{-1}$) was sprayed 2–3 mL onto the leaves using a 10 mL plastic sprinkling can, and hornbeam leaves were treated with sterile water as the control.

Each of the treatment and control groups contained five leaves, and each treatment consisted of one seedling. All of the seedlings under different treatments were kept in a 25 °C greenhouse with high humidity under natural light conditions, and the development of symptoms was observed daily. The experiments were conducted twice.

To complete Koch's postulates, as previously mentioned, the fungus was reisolated from the margin tissue of the diseased lesions that developed from the inoculated tissue and were identified via molecular and phylogenetic analysis.

### 2.3. Morphological Characteristics

Fresh mycelium blocks were cut from the edge of three-day-old colonies and transferred to fresh PDA medium. After 4 days of incubation in the dark at 25 °C, the colony morphology was observed and recorded.

To observe the morphology of conidia, fresh mycelium pieces were cut off and transferred to fresh potato dextrose broth (PDB) supplemented with 100 mg/L ampicillin sodium. Then, the PDB bottles containing the mycelium pieces were placed on a shaking table and shaken at a rotating speed of 200 rpm in the dark at a temperature of 25 °C. After 2 days, the culture solution was collected and filtered with sterile filter cloths to collect the conidia. Appressoria were induced via cultivation on the surface of a hydrophobic coverslip [39]. Asci or ascospores were obtained from the ascomata that grew for 2–3 weeks on PDA or SNA in darkness at 25 °C. Then, each structure was observed to generate 30 measurements using a ZEISS Axio Imager A2m microscope (ZEISS), and the size of each structure was measured using the cross-assay method [40].

### 2.4. Phylogenetic Analysis

Fungal hyphae were collected from fresh colonies using sterilized scalpels. Genomic DNA was extracted using a CTAB Extraction Solution Kit (Leagene Biotechnology, Beijing, China). Then, all of the DNA extracts were stored at −20 °C for subsequent use.

Six nuclear gene regions were amplified and sequenced, including the ITS, CAL, GAPDH, TUB2, ACT, and CHS-1 regions. The primers and PCR conditions are shown in Table 1. Amplification was performed in an Eppendorf Nexus Thermal Cycler (Eppendorf) in a volume of 50 µL, which consisted of 4 µL of genomic DNA, 2 µL of forward/reverse primer (0.01 nmol/µL), 25 µL of 2× Green Taq Mix (Vazyme, Nanjing), and 17 µL of double-distilled H$_2$O. PCR products were sequenced by Sangon Biotech Co., Ltd. (Nanjing, China).

**Table 1.** Primers used in this study, with sequences, PCR conditions, and references.

| Gene | Primer | Sequence (5′-3′) | PCR Conditions | References |
|---|---|---|---|---|
| Internal transcribed spacer (ITS) | ITS1 | CTTGGTCATTTAGAGGAAGTAA | Denaturation for 4 min at 95 °C, followed by 35 cycles of 30 s at 95 °C, 30 s at 52 °C, and 45 s at 72 °C, with a final extension of 7 min at 72 °C | [41,42] |
| | ITS4 | TCCTCCGCTTATTGATATGC | | |
| Calmodulin (CAL) | CL1C | GAATTCAAGGAGGCCTTCTC | Denaturation for 4 min at 95 °C, followed by 35 cycles of 30 s at 95 °C, 30 s at 59 °C, and 45 s at 72 °C, with a final extension of 7 min at 72 °C | [20] |
| | CL2C | CTTCTGCATCATGAGCTGGAC | | |
| Glyceraldehyde-3-phosphate dehydrogenase (GAPDH) | GDF | GCCGTCAACGACCCCTTCATTGA | Denaturation for 4 min at 95 °C, followed by 35 cycles of 30 s at 95 °C, 30 s at 60 °C, and 45 s at 72 °C, with a final extension of 7 min at 72 °C | [43] |
| | GDR | GGGTGGAGTCGTACTTGAGCATGT | | |
| β-tubulin (TUB2) | T1 | AACATGCGTGAGATTGTAAGT | Denaturation for 4 min at 95 °C, followed by 35 cycles of 30 s at 95 °C, 30 s at 55 °C, and 45 s at 72 °C, with a final extension of 7 min at 72 °C | [44,45] |
| | Bt2b | ACCCTCAGTGTAGTGACCCTTGGC | | |
| Actin (ACT) | ACT-512F | ATGTGCAAGGCCGGTTTCGC | Denaturation for 4 min at 95 °C, followed by 35 cycles of 30 s at 95 °C, 30 s at 58 °C, and 45 s at 72 °C, with a final extension of 7 min at 72 °C | [46] |
| | ACT-783R | TACGAGTCCTTCTGGCCCAT | | |
| Chitin synthase 1 (CHS-1) | CHS-79F | TGGGGCAAGGATGCTTGGAAGAAG | Denaturation for 4 min at 95 °C, followed by 35 cycles of 30 s at 95 °C, 30 s at 58 °C, and 45 s at 72 °C, with a final extension of 7 min at 72 °C | [46] |
| | CHS-345R | TGGAAGAACCATCTGTGAGAGTTG | | |
| Glutamine synthetase (GS) | GSF | ATGGCCGAGTACATCTGG | Denaturation for 4 min at 95 °C, followed by 35 cycles of 30 s at 95 °C, 30 s at 59 °C, and 45 s at 72 °C, with a final extension of 7 min at 72 °C | [47] |
| | GSR | GAACCGTCGAAGTTCCAC | | |
| Apn2- Mat1-2 intergenic spacer (ApMat) | CgDL-F6 | AGTGGAGGTGCGGGACGTT | Denaturation for 4 min at 95 °C, followed by 35 cycles of 30 s at 95 °C, 30 s at 58 °C, and 45 s at 72 °C, with a final extension of 7 min at 72 °C | [48] |
| | CgMAT1F2 | TGATGTATCCCGACTACCG | | |

The sequences were analyzed using MAFFT [49] in PhyloSuite v. 1.2.2 [50] and manually trimmed to ensure maximum sequence similarity.

Maximum likelihood (ML) analysis and Bayesian inference (BI) analysis were used to mutually corroborate the phylogenetic reconstructions. IQ-TREE v. 1.6.8 [51] was used for inferring the ML phylogenies under the edge-linked partition model for 100,000 ultrafast bootstraps. MrBayes v. 3.2.6 [52] was used for inferring BI phylogenies, and the initial quarter of the sampled data was discarded as burn-in. ModelFinder [53] was used to select the best-fit model on the basis of the Akaike information criterion (AIC). According to the AIC, the best-fitting model for ML analysis was GTR + F + I + G4, with 1,000,000 ultrafast [54] bootstrap replicates determining the branch stability, while the model for BI analysis was GTR + F + I + G4 under 2 parallel runs of 1,000,000 generations. The phylogenetic tree was viewed by FigTree v. 1.4.4.

### 3. Results

*3.1. Field Survey and Symptoms in the Field*

The field survey was investigated in Xuzhou Urban Garden Company (34.28° N, 118.03° E) in October 2021 and August 2022 in Xuzhou, Jiangsu Province. There were about 5000 European hornbeam in the field, approximately 20% of the European hornbeam showed symptoms of leaf spots, and diseased leaves accounted for approximately 15–20% of the diseased European hornbeam.

Most of the spots were distributed along the edge of the European hornbeam leaves, and the spot wounds tended to expand inward. In addition, some serious disease spots caused leaf shape loss or leaf curling. The spots were brown to dark brown, some areas of the lesion appeared to be grayish-white, and the margin of a part of the lesions appeared as a pale green halo (Figure 1).

*3.2. Fungal Isolation*

A total of 23 fungal strains were isolated from the diseased leaf samples of European hornbeam. Based on ITS sequences, 23 strains belonged to the genus *Colletotrichum*. According to the density of hyphae and the distribution of pigment on the reverse side of colonies, 23 *Colletotrichum* strains were divided into 4 groups, with quantities of 5 (group 1), 12 (group 2), 4 (group 3), and 2 (group 4).
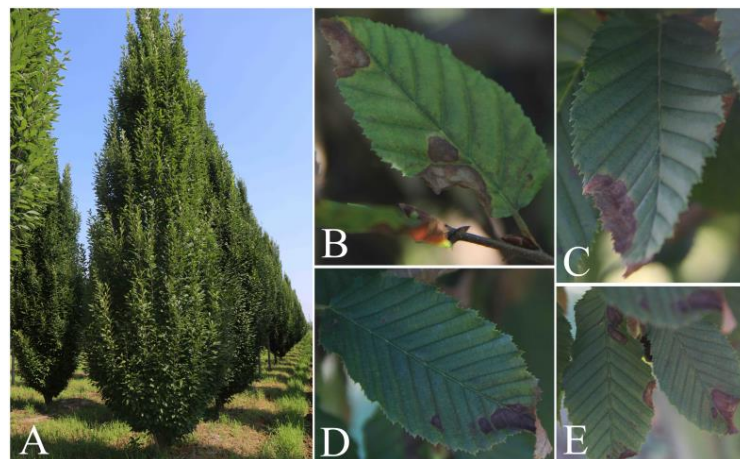
**Figure 1.** European hornbeam leaves with disease symptoms under natural conditions. (**A**) Diseased tree in the field. (**B–E**) Diseased leaves of European hornbeam.
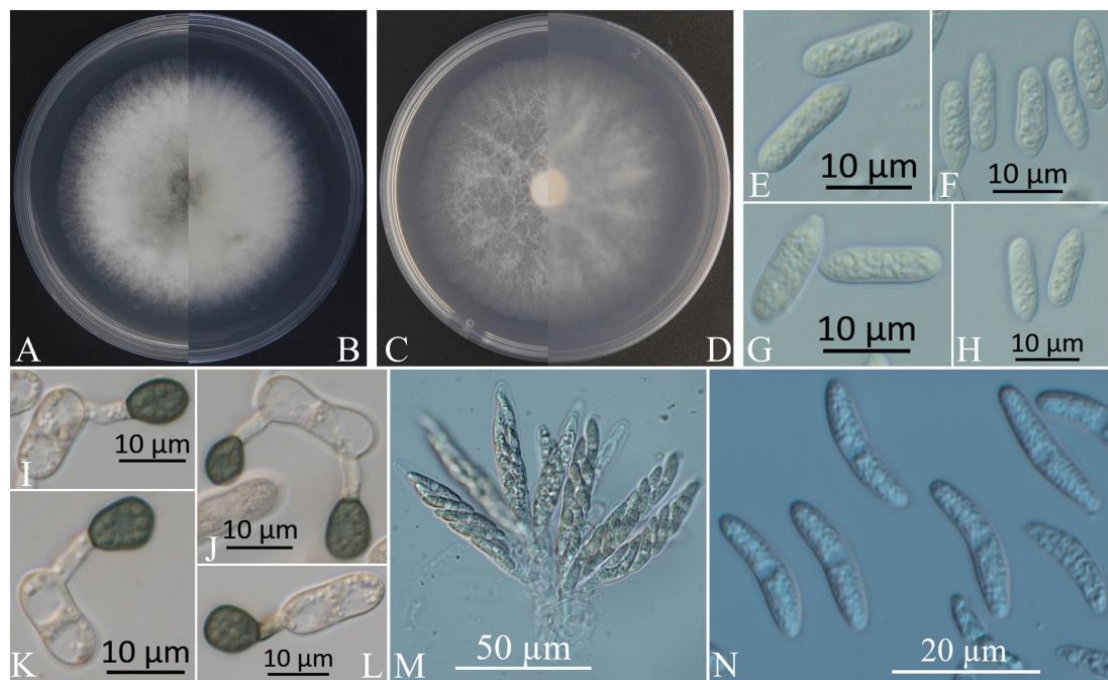
### 3.3. Morphological Characteristics

One representative isolate was selected from each *Colletotrichum* group for further study (XZEC11 from group 1, XZEC21 from group 2, XZEC31 from group 3, and XZEC41 from group 4).

The colonies of XZEC11 isolates produced white aerial hyphae with loose marginal hyphae, and the back of the colonies was light orange-red (Figure 2A,B). The colonies of XZEC21 had fluffy aerial hyphae with loose marginal hyphae, and both sides were all white. The center of the reverse side appeared to be irregular and slightly grayish-green (Figure 3A,B). The aerial hyphae of XZEC31 were compact and raised in the center, and the reverse side was pale orange (Figure 4A,B). The colonies of XZEC41 exhibited fluffy aerial hyphae with loose marginal hyphae, and both sides were all white. The center of the front side was gray, and the reverse side showed blackish-green annular concentric rings (Figure 5A,B).
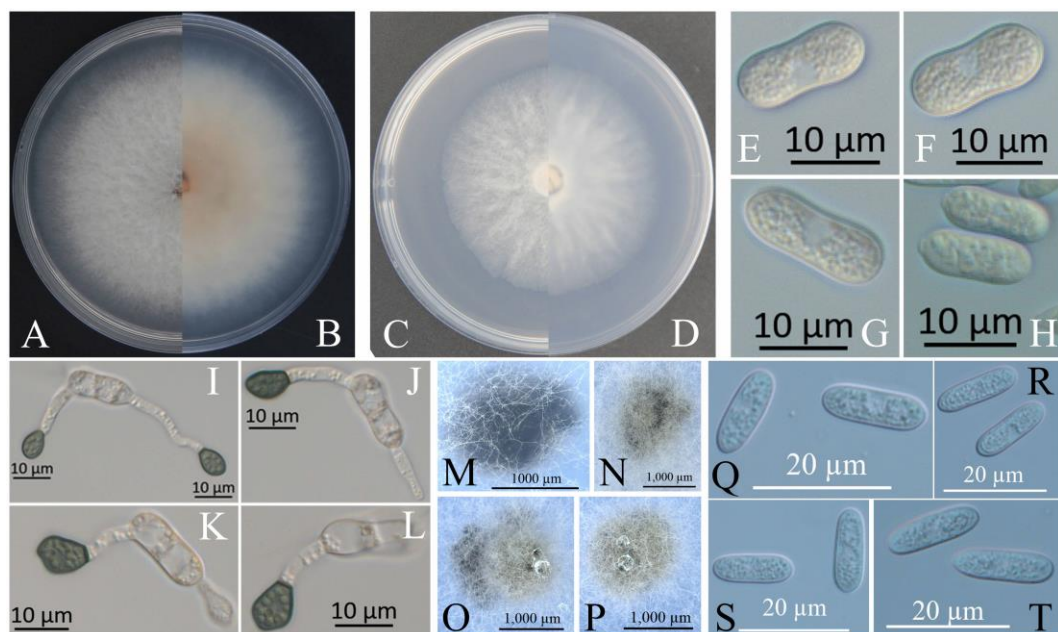


**Figure 2.** Morphological characteristics of XZEC11. (**A,B**) Front and reverse views of 4-day-old fungus on PDA, respectively. (**C,D**) Front and reverse view of 4-day-old fungus on SNA, respectively. (**E–H**) Conidia. (**I–L**) Appressoria. (**M–P**) Ascomata developed in or on SNA after cultivation for 2–3 weeks. (**Q–T**) Ascospores. Scale bars: (**E–L**) = 10 μm; (**M–P**) = 1000 μm; (**Q–T**) = 20 μm.

**Figure 3.** Morphological characteristics of XZEC21. (**A,B**) Front and reverse views of 4-day-old fungus on PDA, respectively. (**C,D**) Front and reverse views of 4-day-old fungus on SNA, respectively. (**E–H**) Conidia. (**I–L**) Appressoria. (**M**) Asci. (**N**) Ascospores. Scale bars: (**E–L**) = 10 μm; (**M**) = 50 μm; (**N**) = 20 μm.
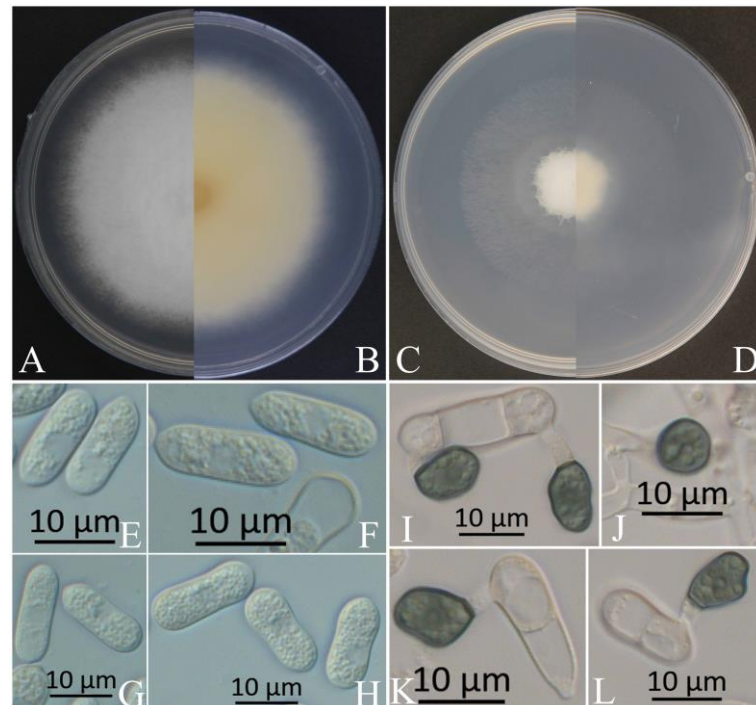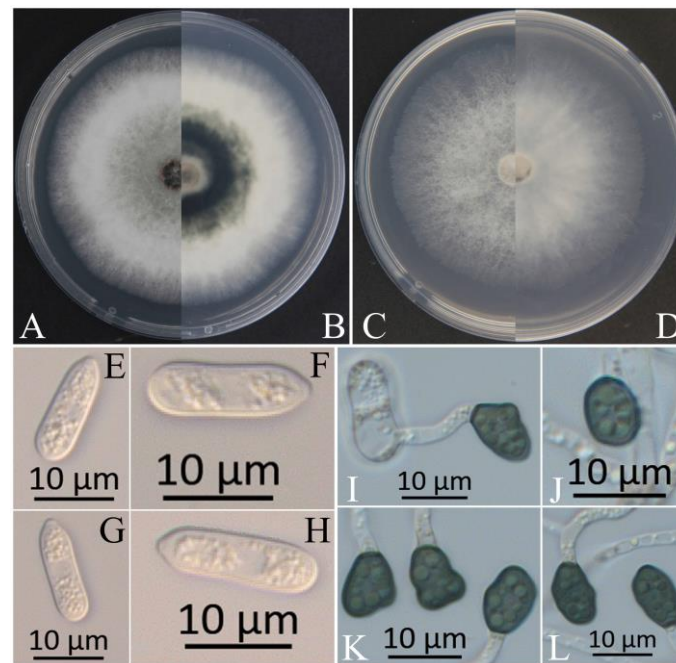


**Figure 4.** Morphological characteristics of XZEC31. (**A,B**) Front and reverse views of 4-day-old fungus on PDA, respectively. (**C,D**) Front and reverse views of 4-day-old fungus on SNA, respectively. (**E–H**) Conidia. (**I–L**) Appressoria. Scale bars: (**E–L**) = 10 μm.

**Figure 5.** Morphological characteristics of XZEC41. (**A**,**B**) Front and reverse views of 4-day-old fungus on PDA, respectively. (**C**,**D**) Front and reverse views of 4-day-old fungus on SNA, respectively. (**E**–**H**) Conidia. (**I**–**L**) Appressoria. Scale bars: (**E**–**L**) = 10 μm.

The colonies of XZEC11, XZEC21, and XZEC41 on SNA produced white, sparse aerial hyphae, and the center area of the colonies of XZEC31 was slightly dense compared with the marginal hyphae; the colonies of XZEC31 produced sparser aerial hyphae than those of the other three *Colletotrichum* groups (Figure 2C,D, Figure 3C,D, Figure 4C,D and Figure 5C,D).

The conidia of the four *Colletotrichum* groups were obtained after shaking cultivation with a rotating speed of 200 rpm in the dark at a temperature of 25 °C. Generally, the structures of the four groups appeared to be cylindrical, straight, and hyaline, and they were all aseptate. Additionally, the conidia of XZEC11 were blunt and rounded at both ends, and the longitudinal middle was slightly concave (Figure 2E–H). The conidia of XZEC21 were thinner than those of the other groups, and one end of the conidia was slightly convex (Figure 3E–H). The conidia of XZEC31 showed a slightly standard semicircle at both ends, and one end was convex (Figure 4E–H). The conidia of XZEC41 had a slightly sharp end and were slightly concave in the middle (Figure 5E–H). The size of each group is shown in Table 2.

**Table 2.** The size of morphological structures of four *Colletotrichum* groups.

| Groups/Isolates | Conidia | Appressoria | Ascospore |
|---|---|---|---|
| XZEC11 | 14.0–18.3 × 5.5–7.8 | 6.8–12.1 × 5.4–8.1 | 14.1–16.9 × 4.4–6.0 |
| XZEC21 | 11.1–14.8 × 3.6–5.7 | 7.1–11.0 × 5.7–8.4 | 19.0–21.8 × 3.7–4.9 |
| XZEC31 | 12.9–17.5 × 5.4–7.3 | 7.0–12.5 × 4.8–8.6 | —— |
| XZEC41 | 12.2–18.6 × 3.8–5.7 | 6.3–12.3 × 5.0–8.3 | —— |

The description of the size is length (μm) × width (μm). The number of each structure observed is 30.

The appressoria of the four *Colletotrichum* groups were induced via cultivation on the surface of the hydrophobic coverslip in darkness at 25 °C for 12 h. The appressoria were all olive green. The shape ranged from nearly round to nearly oval, and irregular shapes were observed. Most of the conidia of the four *Colletotrichum* groups extended from one end to form appressoria, and a few conidia could extend from both ends to form an appressorium (Figures 2I–L, 3I–L, 4I–L and 5I–L). The sizes of the appressoria of the four *Colletotrichum* groups were similar (Table 2).

The ascomata developed on the surface of the colony or under the mycelium, and sterile blades were used to pick the ascomata out of the colony and cut them into pieces to obtain the asci and ascospores. The ascomata of XZEC11 were irregular, and the ascomata produced in the medium were black, while those produced on the surface of the medium were brown (Figure 2M–P). The ascospores of XZEC11 were aseptate, spindle-shaped, slightly curved, and with round ends (Figure 2Q–T); the ascospores of XZEC21 were hyaline, one-celled, and aseptate (Figure 3N). The asci of XZEC21 were clavate, thin-walled, and eight-spored (Figure 3M).

### 3.4. Pathogenicity Tests

For each *Colletotrichum* group, one representative isolate was selected for the pathogenicity test (XZEC11 from group 1, XZEC21 from group 2, XZEC31 from group 3, and XZEC41 from group 4). Four isolates of *Colletotrichum* were pathogenic, and the inoculated European hornbeam leaves showed lesions similar to the previous symptoms that were observed naturally; nevertheless, the controls remained healthy 10 days after inoculation. Most of the lesions occurred at the edge of the leaves, and a few occurred in some central areas of the leaves (Figure 6). According to the appearance of the lesions, lesions caused by XZEC1 and XZEC4 were scattered, and their area was small. Lesions caused by XZEC31 were mainly distributed along the edge of leaves with a long and narrow shape, and some infected areas of leaves were missing. Lesions caused by XZEC21 were mainly distributed along the edge of leaves and were wider than those of XZEC31.
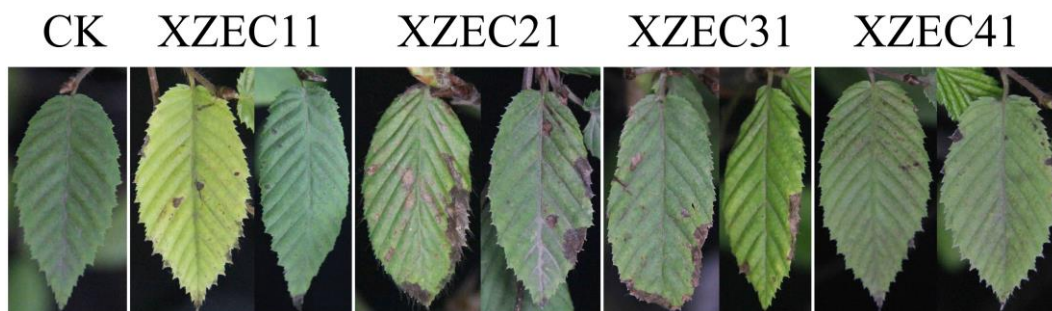


**Figure 6.** Symptoms on European hornbeam leaves 10 days after inoculation with spore suspensions ($10^6$ conidia/mL) of XZEC11, XZEC21, XZEC31, and XZEC41.

### 3.5. Phylogenetic Analysis

Eleven representative *Colletotrichum* strains (three strains of group 1, three strains of group 2, three strains of group 3, and two strains of group 4) were selected for phylogenetic analysis on the basis of the sequences of the six nuclear gene regions. The sequences of the 11 *Colletotrichum* isolates were deposited in GenBank (Table 3). The sequences of the 6 fragments of these 11 *Colletotrichum* isolates were concatenated, and the concatenated matrix consisted of 2837 nucleotide characteristics, viz., ACT: 1–265, ApMat: 266–998, CAL: 999–1650, CHS: 1651–1901, GAPDH: 1902–2156, GS: 2157–3072, ITS: 3073–3618, and TUB: 3619–4349. The sequences of 51 strains of the genus *Colletotrichum* were used to construct a phylogenetic tree, with *Colletotrichum hippeastri* (CBS 241.78) included as the outgroup. The GenBank accession numbers of the 51 sequences of *Colletotrichum* are shown in Table 3.

**Table 3.** Sequences of *Colletotrichum* species used in this study.

| Species, (Culture/Isolate Number [a]) | Country, Host | GenBank Accession Number [b] | | | | | | | |
|---|---|---|---|---|---|---|---|---|---|
| | | ITS | CAL | GAPDH | TUB2 | ACT | CHS-1 | GS | ApMat |
| *C. aenigma* (**ICMP 18608**) | Israel, *Persea americana* | JX010244 | JX009683 | JX010044 | JX010389 | JX009443 | JX009774 | JX010078 | KM360143 |
| *C. aenigma* (ICMP 18686) | Japan, *Pyrus pyrifolia* | JX010243 | JX009684 | JX009913 | JX010390 | JX009519 | JX009789 | JX010079 | — |
| *C. aenigma* (XZEC31 [c]) | China, *Carpinus betulus* | OQ352860 | OQ427912 | OQ427918 | OQ427921 | OQ427909 | OQ427915 | OQ695544 | OQ695541 |
| *C. aenigma* (XZEC32) | China, *C. betulus* | OQ352861 | OQ427913 | OQ427919 | OQ427922 | OQ427910 | OQ427916 | OQ695545 | OQ695542 |
| *C. aenigma* (XZEC33) | China, *C. betulus* | OQ352862 | OQ427914 | OQ427920 | OQ427923 | OQ427911 | OQ427917 | OQ695546 | OQ695543 |
| *C. aeschynomenes* (**ICMP 17673**) | USA, *Aeschynomene virginica* | JX010176 | JX009721 | JX009930 | JX010392 | JX009483 | JX009799 | JX010081 | — |
| *C. alatae* (**CBS 304.67**) | India, *Dioscorea alata* | JX010190 | JX009738 | JX009990 | JX010383 | JX009471 | JX009837 | JX010065 | KC888932 |
| *C. alatae* (ICMP 18122) | Nigeria, *Dioscorea alata* | JX010191 | JX009739 | JX010011 | JX010449 | JX009470 | JX009846 | JX010136 | — |
| *C. alienum* (ICMP 18691) | Australia, *Persea americana* | JX010217 | JX009664 | JX010018 | JX010385 | JX009580 | JX009754 | JX010074 | — |
| *C. alienum* (**ICMP 12071**) | New Zealand, *Malus domestica* | JX010251 | JX009654 | JX010028 | JX010411 | JX009572 | JX009882 | JX010101 | KM360144 |
| *C. alienum* (ICMP 18621) | New Zealand, *Persea americana* | JX010246 | JX009657 | JX009959 | JX010386 | JX009552 | JX009755 | JX010075 | — |
| *C. asianum* (ICMP 18696) | Australia, *Mangifera indica* | JX010192 | JX009723 | JX009915 | JX010384 | JX009576 | JX009753 | JX010073 | — |
| *C. asianum* (**ICMP 18580**) | Thailand, *Coffea arabica* | FJ972612 | FJ917506 | JX010053 | JX010406 | JX009584 | JX009867 | JX010096 | FR718814 |
| *C. chrysophilum* (AFK22) | USA, Apple/Honeycrisp | MN625456 | MN622857 | MN632505 | MN622866 | — | — | MN622843 | MN622875 |
| *C. chrysophilum* (C53, L53) | Uruguay, Apple/Galaxy | MZ562285 | MZ562249 | MG491675 | MG491716 | — | — | MZ562258 | MZ562276 |
| *C. chrysophilum* (CMM 4352) | Brazil, Musa sp. | KX094254 | KX094064 | KX094184 | KX094286 | — | — | KX094205 | KX094326 |
| *C. chrysophilum* (MANE 5) | Brazil, Apple/Gala | KT806271 | MZ595288 | KT806294 | KT806281 | — | — | MZ595299 | MZ595266 |
| *C. fructicola* (ICMP 18120) | Nigeria, *Dioscorea alata* | JX010182 | JX009670 | JX010041 | JX010401 | JX009436 | JX009844 | JX010091 | — |
| *C. fructicola* (CBS 125395) | Panama, *Theobroma cacao* | JX010172 | JX009666 | JX009992 | JX010408 | JX009543 | JX009873 | JX010098 | — |
| *C. fructicola* (**ICMP 18581**) | Thailand, *Coffea arabica* | JX010165 | FJ917508 | JX010033 | JX010405 | FJ907426 | JX009866 | JX010095 | JQ807838 |
| *C. fructicola* (ICMP 18727) | USA, *Fragaria × ananassa* | JX010179 | JX009682 | JX010035 | JX010394 | JX009565 | JX009812 | JX010083 | — |
| *C. fructicola* (XZEC21 [c]) | China, *C. betulus* | OQ352857 | OQ427882 | OQ427888 | OQ427891 | OQ427879 | OQ427885 | OQ695538 | OQ695535 |
| *C. fructicola* (XZEC22) | China, *C. betulus* | OQ352858 | OQ427883 | OQ427889 | OQ427892 | OQ427880 | OQ427886 | OQ695539 | OQ695536 |
| *C. fructicola* (XZEC23) | China, *C. betulus* | OQ352859 | OQ427884 | OQ427890 | OQ427893 | OQ427881 | OQ427887 | OQ695540 | OQ695537 |
| *C. gloeosporioides* (**IMI 356878**) | Italy, *Citrus sinensis* | JX010152 | JX009731 | JX010056 | JX010445 | JX009531 | JX009818 | JX010085 | JQ807843 |
| *C. gloeosporioides* (ICMP 12939) | New Zealand, *Citrus* sp. | JX010149 | JX009728 | JX009931 | — | JX009462 | JX009747 | — | — |

**Table 3.** *Cont.*

| Species, (Culture/Isolate Number [a]) | Country, Host | GenBank Accession Number [b] | | | | | | | |
|---|---|---|---|---|---|---|---|---|---|
| | | ITS | CAL | GAPDH | TUB2 | ACT | CHS-1 | GS | ApMat |
| *C. gloeosporioides* (ICMP 12066) | New Zealand, *Ficus* sp. | JX010158 | JX009734 | JX009955 | — | JX009550 | JX009888 | — | — |
| *C. gloeosporioides* (ICMP 18730) | New Zealand, *Citrus* sp. | JX010157 | JX009737 | JX009981 | — | JX009548 | JX009861 | — | — |
| *C. gloeosporioides* (ICMP 18678) | USA, *Pueraria lobata* | JX010150 | JX009733 | JX010013 | — | JX009502 | JX009790 | — | — |
| *C. gloeosporioides* (XZEC11 [c]) | China, *C. betulus* | OQ352863 | OQ427897 | OQ427903 | OQ427906 | OQ427894 | OQ427900 | OQ695532 | OQ695529 |
| *C. gloeosporioides* (XZEC12) | China, *C. betulus* | OQ352864 | OQ427898 | OQ427904 | OQ427907 | OQ427895 | OQ427901 | OQ695533 | OQ695530 |
| *C. gloeosporioides* (XZEC13) | China, *C. betulus* | OQ352865 | OQ427899 | OQ427905 | OQ427908 | OQ427896 | OQ427902 | OQ695534 | OQ695531 |
| *C. hippeastri* (CBS 241.78) | The Netherlands, *Hippeastrum* sp. | JX010293 | JX009740 | JX009932 | — | JX009485 | JX009838 | — | — |
| *C. horii* (ICMP 12942) | New Zealand, *Diospyros kaki* | GQ329687 | JX009603 | GQ329685 | JX010375 | JX009533 | JX009748 | JX010072 | — |
| *C. horii* (**NBRC 7478**) | Japan, *Diospyros kaki* | GQ329690 | JX009604 | GQ329681 | JX010450 | JX009438 | JX009752 | JX010137 | — |
| *C. horii* (ICMP 17968) | China, *Diospyros kaki* | JX010212 | JX009605 | GQ329682 | JX010378 | JX009547 | JX009811 | JX010068 | — |
| *C. musae* (IMI 52264) | Kenya, *Musa sapientum* | JX010142 | JX009689 | JX010015 | JX010395 | JX009432 | JX009815 | JX010084 | — |
| *C. musae* (**CBS 116870**) | USA, *Musa* sp. | JX010146 | JX009742 | JX010050 | HQ596280 | JX009433 | JX009896 | JX010103 | KC888926 |
| *C. noveboracense* (AFKH109) | USA, Apple/Idared | MN646685 | MN640566 | MN640567 | MN640569 | — | — | MN640568 | MN640564 |
| *C. noveboracense* (PMBrms-1) | USA, Apple | MN715324 | MN741056 | MN741087 | MN741064 | — | — | MN741100 | MN741075 |
| *C. nupharicola* (CBS 469.96) | USA, *Nuphar lutea* subsp. *Polysepala* | JX010189 | JX009661 | JX009936 | JX010397 | JX009486 | JX009834 | JX010087 | — |
| *C. nupharicola* (**CBS 470.96**) | USA, *Nuphar lutea* subsp. *Polysepala* | JX010187 | JX009663 | JX009972 | JX010398 | JX009437 | JX009835 | JX010088 | JX145319 |
| *C. queenslandicum* (**ICMP 1778**) | Australia, *Carica papaya* | JX010276 | JX009691 | JX009934 | JX010414 | JX009447 | JX009899 | JX010104 | KC888928 |
| *C. queenslandicum* (ICMP 18705) | Fiji, *Coffea* sp. | JX010185 | JX009694 | JX010036 | JX010412 | JX009490 | JX009890 | JX010102 | — |
| *C. salsolae* (**ICMP 19051**) | Hungary, *Salsola tragus* | JX010242 | JX009696 | JX009916 | JX010403 | JX009562 | JX009863 | JX010093 | KC888925 |
| *C. salsolae* (CBS 119296) | Hungary, *Glycine max* (inoculated) | JX010241 | JX009695 | JX009917 | — | JX009559 | JX009791 | — | — |
| *C. siamense* (**ICMP 18578**) | Thailand, *Coffea arabica* | JX010171 | FJ917505 | JX009924 | JX010404 | FJ907423 | JX009865 | JX010094 | — |
| *C. siamense* (ICMP 17795) | USA, *Malus domestica* | JX010162 | JX009703 | JX010051 | JX010393 | JX009506 | JX009805 | JX010082 | — |

**Table 3.** *Cont.*

| Species, (Culture/Isolate Number [a]) | Country, Host | GenBank Accession Number [b] | | | | | | | |
|---|---|---|---|---|---|---|---|---|---|
| | | ITS | CAL | GAPDH | TUB2 | ACT | CHS-1 | GS | ApMat |
| *C. siamense* (XZEC41 [c]) | China, *C. betulus* | OQ352866 | OQ427927 | OQ427933 | OQ427936 | OQ427924 | OQ427930 | OQ695549 | OQ695547 |
| *C. siamense* (XZEC42) | China, *C. betulus* | OQ352867 | OQ427928 | OQ427934 | OQ427937 | OQ427925 | OQ427931 | OQ695550 | OQ695548 |
| *C. theobromicola* (ICMP 17895) | Mexico, *Annona diversifolia* | JX010284 | JX009600 | JX010057 | JX010382 | JX009568 | JX009828 | JX010066 | — |
| *C. theobromicola* (**CBS 124945**) | Panama, *Theobroma cacao* | JX010294 | JX009591 | JX010006 | JX010447 | JX009444 | JX009869 | JX010139 | KC790726 |
| *C. tropicale* (MAFF 239933) | Japan, *Litchi chinensis* | JX010275 | JX009722 | JX010020 | JX010396 | JX009480 | JX009826 | JX010086 | — |
| *C. tropicale* (**CBS 124949**) | Panama, *Theobroma cacao* | JX010264 | JX009719 | JX010007 | JX010407 | JX009489 | JX009870 | JX010097 | KC790728 |
| *C. xanthorrhoeae* (**BRIP 45094**) | Australia, *Xanthorrhoea preissii* | JX010261 | JX009653 | JX009927 | JX010448 | JX009478 | JX009823 | JX010138 | KC790689 |
| *C. xanthorrhoeae* (ICMP 17820) | Australia, *Xanthorrhoea* sp. | JX010260 | JX009652 | JX010008 | — | JX009479 | JX009814 | — | — |

[a]: The number of cultures/isolates in bold represents ex-type strains. ATCC, American Type Culture Collection; BRIP, Plant Pathology Herbarium, Department of Employment, Economic Development and Innovation, Queensland, Australia; CBS, Culture Collection of the Centraalbureau voor Schimmelcultures, Fungal Biodiversity Center, Utrecht, the Netherlands; ICMP, International Collection of Microorganisms from Plants, Auckland, New Zealand; IMI, Culture Collection of CABI Europe UK Centre, Egham, UK; MAFF, MAFF Genebank Project, Ministry of Agriculture, Forestry and Fisheries, Tsukuba, Japan; MFLUCC, Mae Fah Luang University Culture Collection, Chiang Rai, Thailand; NBRC, Biological Resource Center, National Institute of Technology and Evaluation, Japan. *C. hippeastri* (CBS 241.78) was added as an outgroup. [b]: ITS, internal transcribed spacer gene; CAL, partial calmodulin gene; CHS-1, partial chitin synthase; GAPDH, partial glyceraldehyde 3-phosphate dehydrogenase gene; ACT, partial actin gene; TUB2, partial beta-tubulin 2 gene; [c]: isolates used for morphological and biological analysis and pathogenicity tests.

ML and BI analyses produced similar topologies, providing statistical support for the evolutionary relationships of fungal isolates, and a consensus tree with clade support from bootstrap proportions (BPs) and Bayesian posterior probabilities (BPPs) was generated (Figure 7). As shown in Figure 7, 11 *Colletotrichum* strains were placed in 4 different clades with high support values: 3 strains of group 1 were clustered with *C. gloeosporioides* (BP/BPP = 100%/1), 3 strains of group 2 were clustered with *C. fructicola* (BP/BPP = 98%/0.98), 3 strains of group 3 were clustered with *C. aenigma* (BP/BPP = 99%/1), and 2 strains of group 4 were clustered with *C. siamense* (BP/BPP = 99%/1).
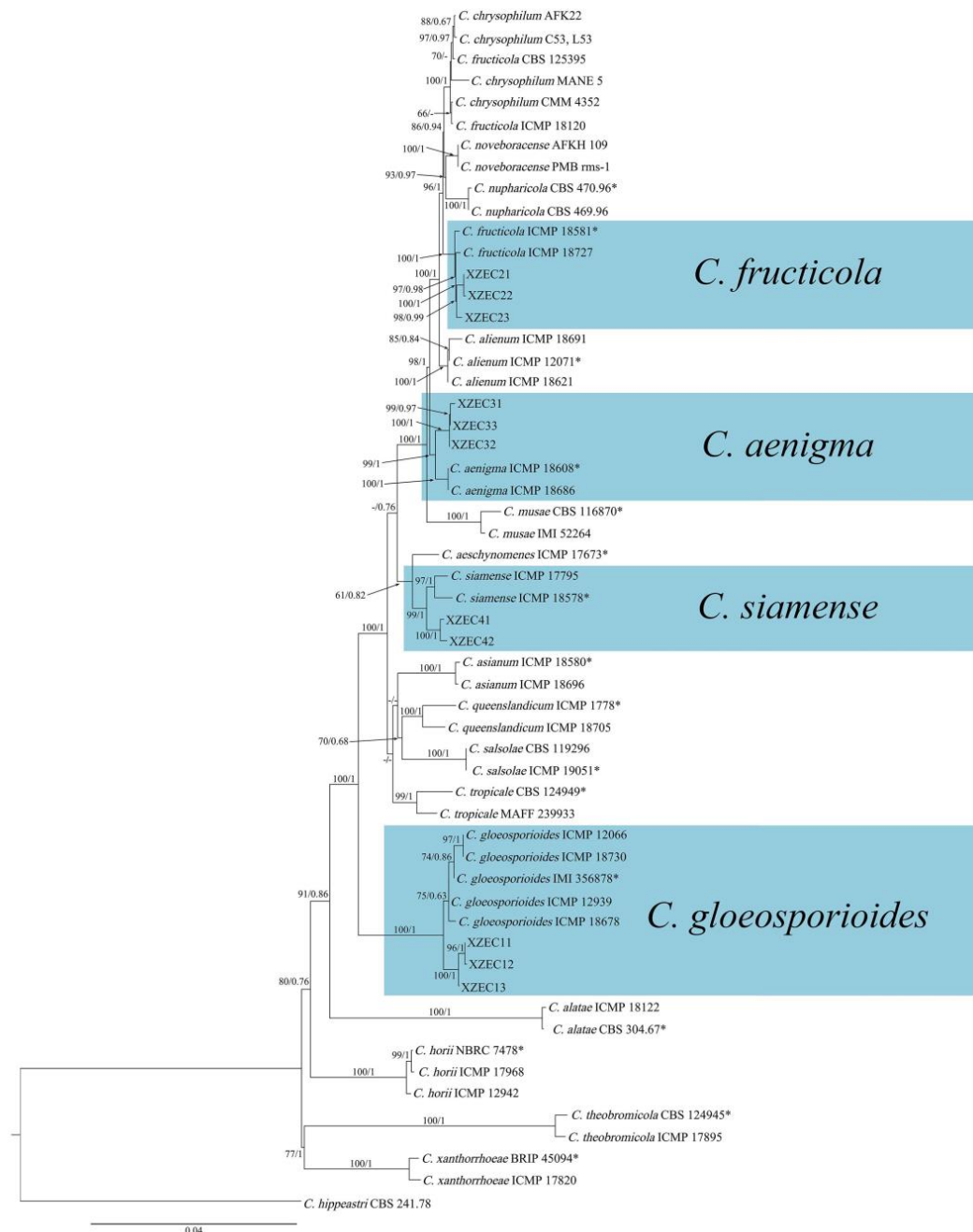


**Figure 7.** Phylogenetic tree generated with the concatenated sequences of the ITS, ACT, ApMat, CAL, CHS−1, GAPDH, GS, and TUB2 genes using maximum likelihood analysis. The tree generated by Bayesian inference had a similar topology. Bootstrap support values above 60% (before the slash marks) and Bayesian posterior probabilities above 0.60 (after the slash marks) are given at each node (BP/BPP). *Colletotrichum hippeastri* (CBS 241.78) was used as an outgroup. Ex-type strains are marked with (*).

## 4. Discussion

A graceful appearance with strong phenotypic plasticity and excellent technical properties of timber gives European hornbeams an important role in urban landscaping and economy. However, leaf spot deteriorates the leaf appearance and affects apical dominance, reducing the quality of wood [55]. In this study, *C. gloeosporioides*, *C. fructicola*, *C. aenigma*, and *C. siamense* were identified as the causal agents of leaf spot on European hornbeam.

Generally speaking, the morphological structure will be identified initially to determine the genus of *Colletotrichum*. In early studies, most of the identification of the *Colletotrichum* species was based on the shape of the conidia [56,57]. The size of the conidia of *C. gloeosporioides* in this study was similar to that reported by Huang et al. [58], Kim et al. [59], and Chen et al. [60], but larger than that reported by Chen et al. [61]. The conidia of *C. siamense* were similar to those reported by Kim et al. [59] and Cao et al. [62], but smaller than those reported by Zhang et al. [63]. The conidia of *C. aenigma* were similar to those reported by Zheng et al. [64] but larger than those reported by Wang et al. [65]. The conidia of *C. fructicola* were similar to those reported by Cai et al. [66] and Huang et al. [58] but shorter than those reported by Costa et al. [67] and Zheng et al. [64]. Other structures, such as appressoria, also exhibit various degrees of difference. This phenomenon in which the sizes of the same structure are not similar could be because of different growth conditions or a loss or change under repeated subculturing [20], similar to the results reported for the asci and ascospores of *C. siamense* and *C. aenigma*, which we failed to induce in this study. Significantly, we isolated *C. aenigma* from *Acer rubrum* in 2020 in the same nursery in Xuzhou [68], and the method of inducing asci and ascospores was developed during the cultivation of *C. aenigma* (2020). Except for asci and ascospores, the colonies of the two *C. aenigma* species were not quite the same (Figure 8). The colonies of *C. aenigma* (2020) were relatively flat, with a relatively fluffy texture. The middle area of *C. aenigma* colonies (2022) was raised, the height dropped gradually from the middle to the edge, and the texture was relatively tight.
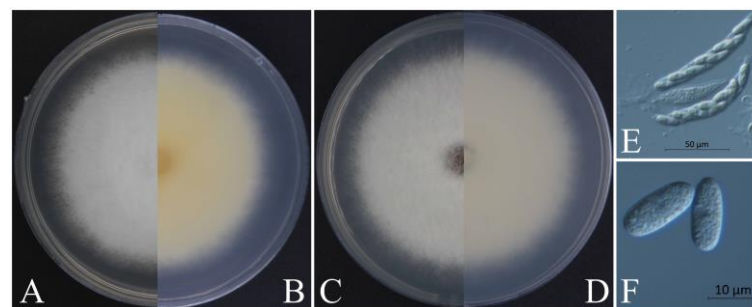


**Figure 8.** Morphological characteristics of *Colletotrichum aenigma*. (**A,B**) Front and reverse views of 4-day-old fungus on PDA of *C. aenigma* (2022), respectively. (**C,D**) Front and reverse views of 4-day-old fungus on SNA of *C. aenigma* (2020), respectively. (**E**) Asci of *C. aenigma* (2020), scale bar = 50 μm. (**F**) Ascospores of *C. aenigma* (2020), scale bar = 10 μm.

During the cultivating of these two *Colletotrichum aenigma*, we used the same PDA medium with the same formula, cultivated them in the same incubator in the darkness at 25 °C, and the positions in the incubator were also very close. However, despite this, the colony morphology and the ability to produce asci and ascospores changed. It is confusing that the morphology of the same *Colletotrichum* species changed just because of the different hosts. Therefore, it is not accurate to identify the *Colletotrichum* species only from morphology, even if it is a 100% identical species. So, more accurate identification methods are needed to distinguish the *Colletotrichum* species, such as multi-gene-combined phylogenetic analysis.

According to the previous literature, ACT, CHS-1, GAPDH, HIS3, ITS, and TUB2 could be used to classify the majority of the *Colletotrichum* species [6], and three additional loci (ApMat, CAL, and GS) have been used for the *C. gloeosporioides* species complex [20,69].

Five conventional genes (ACT, CHS-1, GAPDH, ITS, and TUB2), four specific genes (ApMat, CAL, and GS), and one additional specific gene (APN2) were used in this study, and four species in this study were separated from the *C. gloeosporioides* species complex. The combined phylogenetic tree was consistent with trees presented in other studies [61,70–72].

Due to its strong environmental adaptability, the *Colletotrichum* species can cause leaf spot and fruit diseases with huge losses in agricultural and forestry production worldwide [21,65,73–82]. Furthermore, changes in the climate, human activities, and other factors may cause fungi host jumping within the plants in the nursery [83]. It is very likely that *C. aenigma*, which we isolated in 2020 and 2022, has experienced this, and maybe *C. aenigma* and the other three species also jumped to the other hosts (except for *Acer rubrum* and European hornbeams), though we have not found this yet. Therefore, more reports about local leaf spot diseases caused by *Colletotrichum* species may be produced in the future.

## 5. Conclusions

In conclusion, this study identified *C. gloeosporioides*, *C. fructicola*, *C. aenigma*, and *C. siamense* as the pathogens causing leaf blight on European hornbeam, posing a new and emerging threat to European hornbeam. This research represents the first detailed study of the pathogenicity, morphology, and phylogeny of four *Colletotrichum* species on European hornbeam in China. Further research exploring the infection cycle of this emerging disease in European hornbeam remains to be conducted, and strategies for the control of this new pathological system should be identified.

**Author Contributions:** Conceptualization, F.-M.C.; methodology, Y.-H.Q.; software, Y.-H.Q. and C.-N.Z.; validation, Y.-H.Q.; formal analysis, Y.-H.Q. and C.-N.Z.; investigation, Y.-F.M. and Y.-H.Q.; resources, F.-M.C.; data curation, Y.-H.Q.; writing—original draft preparation, Y.-H.Q. and C.-N.Z.; writing—review and editing, M.L. and H.L.; visualization, Y.-H.Q.; supervision, F.-M.C.; project administration, F.-M.C.; funding acquisition, F.-M.C. All authors have read and agreed to the published version of the manuscript.

**Institutional Review Board Statement:** Not applicable for studies not involving humans or animals.

**Informed Consent Statement:** Not applicable.

**Data Availability Statement:** All data generated or analyzed during this study are included in this article.

**Conflicts of Interest:** The authors declare no conflict of interest.

## References

1. Abdi, E.; Majnounian, B.; Rahimi, H.; Zobeiri, M. Distribution and tensile strength of Hornbeam (*Carpinus betulus*) roots growing on slopes of Caspian Forests, Iran. *J. For. Res.* **2009**, *20*, 105–110. [CrossRef]
2. Kiaei, M. Effect of site and elevation on wood density and shrinkage and their relationships in *Carpinus betulus*. *For. Stud. China* **2012**, *14*, 229–234. [CrossRef]
3. Rocchi, F.; Quaroni, S.; Sardi, P.; Saracchi, M. Studies on Anthostoma decipiens involved in *Carpinus betulus* decline. *J. Plant Pathol.* **2010**, *92*, 637–644. [CrossRef]
4. Cieckiewicz, E.; Angenot, L.; Gras, T.; Kiss, R.; Frédérich, M. Potential anticancer activity of young *Carpinus betulus* leaves. *Phytomedicine* **2012**, *19*, 278–283. [CrossRef] [PubMed]
5. Sheng, Q.Q.; Fang, X.Y.; Zhu, Z.L.; Xiao, W.; Wang, Z.Z.; Ding, G.; Zhao, L.G.; Li, Y.J.; Yu, P.; Ding, Z.B.; et al. Seasonal variation of pheophorbide a and flavonoid in different organs of two *Carpinus* species and its correlation with immunosuppressive activity. *In Vitro Cell. Dev. Biol. Anim.* **2016**, *52*, 654–661. [CrossRef] [PubMed]
6. Liu, F.; Ma, Z.; Hou, L.; Diao, Y.; Wu, W.; Damm, U.; Song, S.; Cai, L. Updating species diversity of *Colletotrichum*, with a phylogenomic overview. *Stud. Mycol.* **2022**, *101*, 1–56. [CrossRef]
7. Dean, R.; Van Kan, J.A.L.; Pretorius, Z.A.; Hammond-Kosack, K.E.; Di Pietro, A.; Spanu, P.D.; Rudd, J.J.; Dickman, M.; Kahmann, R.; Ellis, J.; et al. The Top 10 fungal pathogens in molecular plant pathology. *Mol. Plant Pathol.* **2012**, *13*, 414–430. [CrossRef]
8. Cannon, P.F.; Buddie, A.G.; Bridge, P.D. The typification of *Colletotrichum gloeosporioides*. *Mycotaxon* **2008**, *104*, 189–204.

9. O'Connell, R.J.; Thon, M.R.; Hacquard, S.; Amyotte, S.G.; Kleemann, J.; Torres, M.F.; Damm, U.; Buiate, E.A.; Epstein, L.; Alkan, N. Lifestyle transitions in plant pathogenic *Colletotrichum* fungi deciphered by genome and transcriptome analyses. *Nat. Genet.* **2012**, *44*, 1060–1065. [CrossRef]

10. Guarro, J.; Svidzinski, T.E.; Zaror, L.S.; Forjaz, M.H.; Gené, J.; Fischman, O. Subcutaneous hyalohyphomycosis caused by *Colletotrichum gloeosporioides*. *J. Clin. Microbiol.* **1998**, *36*, 3060–3065. [CrossRef]

11. Shiraishi, A.; Araki-Sasaki, K.; Mitani, A.; Miyamoto, H.; Sunada, A.; Ueda, A.; Asari, S.; Zheng, X.; Yamamoto, Y.; Hara, Y. Clinical characteristics of keratitis due to *Colletotrichum gloeosporioides*. *J. Ocul. Pharmacol. Ther.* **2011**, *27*, 487–491. [CrossRef] [PubMed]

12. Du, M.; Schardl, C.L.; Nuckles, E.M.; Vaillancourt, L.J. Using mating-type gene sequences for improved phylogenetic resolution of *Collectotrichum species complexes*. *Mycologia* **2005**, *97*, 641–658. [CrossRef] [PubMed]

13. Damm, U.; Woudenberg, J.H.C.; Cannon, P.F.; Crous, P.W. *Colletotrichum* species with curved conidia from herbaceous hosts. *Fungal Divers.* **2009**, *39*, 45. [CrossRef]

14. Xiang, M.; Zhang, Y.; Liu, X. Research progress on the taxonomy of *Colletotrichum*. *J. Zhongkai Univ. Agric. Eng.* **2017**, *30*, 59–66.

15. Bailey, J.A.; O'Connell, R.J.; Pring, R.J. Infection strategies of *Colletotrichum* species. In *Colletotrichum: Biology, Pathology and Control*; CAB International: Wallingford, UK, 1992.

16. Thaung, M.M. Coelomycete systematics with special reference to *Colletotrichum*. *Mycoence* **2008**, *49*, 345–350. [CrossRef]

17. Sherriff, C.; Whelan, M.J.; Arnold, G.M.; Lafay, J.F.; Brygoo, Y.; Bailey, J.A. Ribosomal DNA Sequence Analysis Reveals New Species Groupings in the Genus *Colletotrichum*. *Exp. Mycol.* **1994**, *18*, 121–138. [CrossRef]

18. Crouch, J.A.; Clarke, B.B.; White Jr, J.F.; Hillman, B.I. Systematic analysis of the falcate-spored graminicolous *Colletotrichum* and a description of six new species from warm-season grasses. *Mycologia* **2009**, *101*, 717–732. [CrossRef]

19. Li, N. *Study on the Species of Anthracnose Pathogens and the Groups Gegetic Diversity*; Sichuan Agricultural University: Chengdu, China, 2012.

20. Weir, B.S.; Johnston, P.R.; Damm, U. The *Colletotrichum gloeosporioides* species complex. *Stud. Mycol.* **2012**, *73*, 115–180. [CrossRef]

21. Zhou, Y.; Ye, R.; Ying, Q.; Zhang, Y.; Zhang, L. First Report of Leaf Spot Caused by *Colletotrichum fructicola* on *Dalbergia hupeana* in China. *Plant Dis.* **2022**, *106*, 1526. [CrossRef]

22. Prihastuti, H.; Cai, L.; Chen, H.; McKenzie, E.; Hyde, K. Characterization of *Colletotrichum* species associated with coffee berries in northern Thailand. *Fungal Divers* **2009**, *39*, 89–109.

23. Shu, J.; Ning, P.; Guo, T.; Tang, L.; Huang, S.; Li, Q.; Mo, J.; Yu, Z.; Hsiang, T. First report of leaf spot caused by *Colletotrichum fructicola* on Callerya speciosa (*Millettia speciosa*) in Guangxi, China. *Plant Dis.* **2020**, *104*, 1–6. [CrossRef]

24. Meetum, P.; Leksomboon, C.; Kanjanamaneesathian, M. First report of *Colletotrichum aenigma* and *C. siamense*, the causal agents of anthracnose disease of dragon fruit in Thailand. *J. Plant Pathol.* **2015**, *97*, 402. [CrossRef]

25. Choi, H.-W.; Lee, Y.; Hong, S. First report of *Colletotrichum aenigma* causing anthracnose on *Sedum kamtschaticum* in Korea. *Plant Dis.* **2017**, *101*, 2150. [CrossRef]

26. Yang, S.; Wang, H.; Yi, Y.; Tan, L. First report that *Colletotrichum aenigma* causes leaf spots on *Camellia japonica* L. in China. *Plant Dis.* **2019**, *103*, 2127. [CrossRef]

27. Tang, S.-F.; Tan, L.-L. First Report of *Colletotrichum gloeosporioides* Causing Leaf Spots on *Rubia cordifolia* in Qingdao, China. *Plant Dis.* **2020**, *104*, 2733. [CrossRef]

28. Riolo, M.; Aloi, F.; Pane, A.; Cara, M.; Cacciola, S.O. Twig and shoot dieback of citrus, a new disease caused by *Colletotrichum* species. *Cells* **2021**, *10*, 449. [CrossRef]

29. Pacheco-Esteva, M.C.; Soto-Castro, D.; Vásquez-López, A.; Tovar-Pedraza, J.M. First report of *Colletotrichum siamense* causing papaya anthracnose in Mexico. *J. Plant Pathol.* **2022**, *104*, 1175. [CrossRef]

30. Krishnan, S.; Kaari, M.; Sawhney, S.; Sheoran, N.; Gautam, R.K.; Mohan Das, M.; Kumar, A. First report of *Colletotrichum siamense* from Andaman and Nicobar Islands causing anthracnose in *chilli*. *J. Plant Pathol.* **2019**, *101*, 767. [CrossRef]

31. Wang, W.; Zhang, J.; Li, J. First report of *Colletotrichum siamense* causing stem tip dieback of Sacha Inchi (*Plukenetia volubilis*) in China. *Plant Dis.* **2020**, *104*, 2726. [CrossRef]

32. Borges, R.C.; Rossato, M.; Santos, M.D.M.; Macedo, M.A.; Fonseca, M.; Boiteux, L.; Reis, A. *Colletotrichum siamense* as a causal agent of leaf anthracnose in seedlings of *Annona muricata* in nurseries from the Federal District, Brazil. *J. Plant Dis. Prot.* **2021**, *128*, 583–588. [CrossRef]

33. Piątek, M. First report of powdery mildew (*Oidium carpini*) on *Carpinus betulus* in Poland. *Plant Pathol.* **2004**, *53*, 246. [CrossRef]

34. Vajna, L. Powdery mildew caused by *Erysiphe carpinicola* on *Carpinus betulus* in Hungary: The first European report. *Plant Pathol.* **2006**, *55*, 575. [CrossRef]

35. Pastircakova, K.; Takamatsu, S.; Shiroya, Y.; Pastircak, M. European hornbeam powdery mildew *Erysiphe arcuata* in Slovakia. *J. Phytopathol.* **2008**, *156*, 597–601. [CrossRef]

36. Chinan, V.-C.; Mânzu, C.C. First report of *Erysiphe arcuata* on *Carpinus betulus* in Romania. *J. Plant Pathol.* **2021**, *103*, 405. [CrossRef]

37. Mao, Y.-F.; Chen, H.; Jin, L.; Wang, M.; Zheng, X.-R.; Chen, F. First Report of Wilt of European Hornbeam (*Carpinus betulus*) Caused by *Fusarium oxysporum* in China. *Plant Dis.* **2021**, *105*, 3759. [CrossRef]

38. Xue, L.H.; Zhang, L.; Yang, X.X.; Huang, X.Q.; Wu, W.X.; Zhou, X.Q.; White, J.F.; Liu, Y.; Li, C.J. Characterization, Phylogenetic Analyses, and Pathogenicity of *Colletotrichum* Species on *Morus alba* in Sichuan Province, China. *Plant Dis.* **2019**, *103*, 2624–2633. [CrossRef]

39. Huang, L.; Li, Q.C.; Zhang, Y.; Li, D.W.; Ye, J.R. *Colletotrichum gloeosporioides* sensu stricto Is a Pathogen of Leaf Anthracnose on Evergreen Spindle Tree (*Euonymus japonicus*). *Plant Dis.* **2016**, *100*, 672–678. [CrossRef]

40. Lin, S.H.; Huang, S.L.; Li, Q.Q.; Hu, C.J.; Fu, G.; Qin, L.P.; Ma, Y.F.; Xie, L.; Cen, Z.L.; Yan, W.H. Characterization of *Exserohilum rostratum*, a new causal agent of banana leaf spot disease in China. *Australas. Plant Pathol.* **2011**, *40*, 246–259. [CrossRef]

41. White, T.J.; Bruns, T.D.; Lee, S.B.; Taylor, J.W. Amplification and Direct Sequencing of Fungal Ribosomal RNA Genes for Phylogenetics. In *PCR—Protocols and Applications—A Laboratory Manual*; Innis, M.A., Gelfand, D.H., Sninsky, J.J., White, T.J., Eds.; Academic Press, Inc.: New York, NY, USA, 1990.

42. Gardes, M.; Bruns, T.D. ITS primers with enhanced specificity for basidiomycetes-application to the identification of mycorrhizae and rusts. *Mol. Ecol.* **1993**, *2*, 113–118. [CrossRef] [PubMed]

43. Templeton, M.D.; Rikkerink, E.H.; Solon, S.L.; Crowhurst, R.N. Cloning and molecular characterization of the glyceraldehyde-3-phosphate dehydrogenase-encoding gene and cDNA from the plant pathogenic fungus *Glomerella cingulata*. *Gene* **1992**, *122*, 225–230. [CrossRef]

44. O'Donnell, K.; Cigelnik, E. Two divergent intragenomic rDNA ITS2 types within a monophyletic lineage of the fungus *Fusarium* are nonorthologous. *Mol. Phylogenetics Evol.* **1997**, *7*, 103–116. [CrossRef] [PubMed]

45. Glass, N.L.; Donaldson, G.C. Development of primer sets designed for use with the PCR to amplify conserved genes from filamentous ascomycetes. *Appl. Environ. Microbiol.* **1995**, *61*, 1323–1330. [CrossRef] [PubMed]

46. Carbone, I.; Kohn, L.M. A method for designing primer sets for speciation studies in filamentous ascomycetes. *Mycologia* **1999**, *91*, 553–556. [CrossRef]

47. Stephenson, S.-A.; Green, J.R.; Manners, J.M.; Maclean, D.J. Cloning and characterisation of glutamine synthetase from Colletotrichum gloeosporioides and demonstration of elevated expression during pathogenesis on Stylosanthes guianensis. *Curr. Genet.* **1997**, *31*, 447–454. [CrossRef] [PubMed]

48. Rojas, E.I.; Rehner, S.A.; Samuels, G.J.; Van Bael, S.A.; Herre, E.A.; Cannon, P.; Chen, R.; Pang, J.; Wang, R.; Zhang, Y. Colletotrichum gloeosporioides sl associated with Theobroma cacao and other plants in Panama: Multilocus phylogenies distinguish host-associated pathogens from asymptomatic endophytes. *Mycologia* **2010**, *102*, 1318–1338. [CrossRef]

49. Katoh, K.; Standley, D.M. MAFFT multiple sequence alignment software version 7: Improvements in performance and usability. *Mol. Biol. Evol.* **2013**, *30*, 772–780. [CrossRef]

50. Zhang, D.; Gao, F.; Jakovlić, I.; Zou, H.; Zhang, J.; Li, W.X.; Wang, G.T. PhyloSuite: An integrated and scalable desktop platform for streamlined molecular sequence data management and evolutionary phylogenetics studies. *Mol. Ecol. Resour.* **2020**, *20*, 348–355. [CrossRef]

51. Nguyen, L.-T.; Schmidt, H.A.; Von Haeseler, A.; Minh, B.Q. IQ-TREE: A fast and effective stochastic algorithm for estimating maximum-likelihood phylogenies. *Mol. Biol. Evol.* **2015**, *32*, 268–274. [CrossRef]

52. Ronquist, F.; Teslenko, M.; Van Der Mark, P.; Ayres, D.L.; Darling, A.; Höhna, S.; Larget, B.; Liu, L.; Suchard, M.A.; Huelsenbeck, J.P. MrBayes 3.2: Efficient Bayesian phylogenetic inference and model choice across a large model space. *Syst. Biol.* **2012**, *61*, 539–542. [CrossRef]

53. Kalyaanamoorthy, S.; Minh, B.Q.; Wong, T.K.; Von Haeseler, A.; Jermiin, L.S. ModelFinder: Fast model selection for accurate phylogenetic estimates. *Nat. Methods* **2017**, *14*, 587–589. [CrossRef]

54. Minh, B.Q.; Nguyen, M.A.T.; Von Haeseler, A. Ultrafast approximation for phylogenetic bootstrap. *Mol. Biol. Evol.* **2013**, *30*, 1188–1195. [CrossRef]

55. Zhang, M.-J.; Zheng, X.-R.; Li, H.; Chen, F.-M. Alternaria alternata, the Causal Agent of a New Needle Blight Disease on Pinus bungeana. *J. Fungi* **2023**, *9*, 71. [CrossRef]

56. Sutton, B.C. Fungi Imperfecti with Pycnidia, Acervuli and Stromata. In *The Coelomycetes*; Commonwealth Mycological Institute: London, UK, 1980.

57. Von Arx, J.A. A revision of the fungi classified as Gloeosporium. In *A Revision of the Fungi Classified as Gloeosporium*; CAB International: Wallingford, UK, 1970.

58. Huang, F.; Chen, G.; Hou, X.; Fu, Y.; Cai, L.; Hyde, K.; Li, H. Colletotrichum species associated with cultivated citrus in China. *Fungal Divers.* **2013**, *61*, 61–74. [CrossRef]

59. Kim, C.H.; Hassan, O.; Chang, T. Diversity, pathogenicity, and fungicide sensitivity of Colletotrichum species associated with apple anthracnose in South Korea. *Plant Dis.* **2020**, *104*, 2866–2874. [CrossRef]

60. Chen, Y.; Qiao, W.; Zeng, L.; Shen, D.; Liu, Z.; Wang, X.; Tong, H. Characterization, pathogenicity, and phylogenetic analyses of Colletotrichum species associated with brown blight disease on Camellia sinensis in China. *Plant Dis.* **2017**, *101*, 1022–1028. [CrossRef] [PubMed]

61. Chen, X.; Dai, D.; Zhao, S.; Shen, Y.; Wang, H.; Zhang, C. Genetic diversity of Colletotrichum spp. causing strawberry anthracnose in Zhejiang, China. *Plant Dis.* **2020**, *104*, 1351–1357. [CrossRef]

62. Cao, X.; Xu, X.; Che, H.; West, J.S.; Luo, D. Eight Colletotrichum species, including a novel species, are associated with areca palm anthracnose in Hainan, China. *Plant Dis.* **2020**, *104*, 1369–1377. [CrossRef] [PubMed]

63. Zhang, Y.; Wang, J.; Yin, C.; Mao, Z.; Shao, Y. First report of Colletotrichum siamense causing Anthracnose on Jasminum mesnyi in China. *Plant Dis.* **2019**, *103*, 2675. [CrossRef]

64. Zheng, X.-r.; Zhang, M.-j.; Shang, X.-l.; Fang, S.-z.; Chen, F.-m. Etiology of Cyclocarya paliurus anthracnose in Jiangsu province, China. *Front. Plant Sci.* **2021**, *11*, 613499. [CrossRef]

65. Wang, Y.; Jia, W.; Zhu, X.; Mi, Z.; Wang, E.; Chang, G.; Yan, S.; Wang, X.; Kong, D.; He, S. First Report of *Colletotrichum aenigma* Causing Anthracnose of tree peony in China. In *Plant Disease*; The American Phytopathological Society (APS): St. Paul, MN, USA, 2022. [CrossRef]

66. Cai, L.; Hyde, K.; Taylor, P.; Weir, B.; Waller, J.; Abang, M.; Zhang, J.; Yang, Y.; Phoulivong, S.; Liu, Z. A polyphasic approach for studying Colletotrichum. *Fungal Divers.* **2009**, *39*, 183–204.

67. Costa, J.; Ramos-Sobrinho, R.; Chaves, T.; Silva, J.; Pinho, D.; Assunção, I.; Lima, G. First report of Colletotrichum fructicola causing anthracnose on Annona leaves in Brazil. *Plant Dis.* **2017**, *101*, 386. [CrossRef]

68. Yuhang, Q.; Xiangrong, z.; Huan, L.; FengMao, C. First Report of Leaf Spot Caused by *Colletotrichum aenigma* on *Acer rubrum* in China. In *Plant Disease*; The American Phytopathological Society (APS): St. Paul, MN, USA, 2022. [CrossRef]

69. Liu, F.; Weir, B.; Damm, U.; Crous, P.W.; Wang, Y.; Liu, B.; Wang, M.; Zhang, M.; Cai, L. Unravelling Colletotrichum species associated with Camellia: Employing ApMat and GS loci to resolve species in the C. gloeosporioides complex. *Pers. Mol. Phylogeny Evol. Fungi* **2015**, *35*, 63–86. [CrossRef]

70. Li, F.; Chen, J.; Chen, Q.; Liu, Z.; Sun, J.; Yan, Y.; Zhang, H.; Bi, Y. Identification, Pathogenicity, and Sensitivity to Fungicide of Colletotrichum Species That Causes Walnut Anthracnose in Beijing. *Agronomy* **2023**, *13*, 214. [CrossRef]

71. Wu, J.; Hu, S.; Ye, B.; Hu, X.; Xiao, W.; Yu, H.; Zhang, C. Diversity and Resistance to Thiophanate-Methyl of Colletotrichum spp. in Strawberry Nursery and the Development of Rapid Detection Using LAMP Method. *Agronomy* **2022**, *12*, 2815. [CrossRef]

72. Chen, Y.; Fu, D.; Wang, W.; Gleason, M.L.; Zhang, R.; Liang, X.; Sun, G. Diversity of Colletotrichum species causing apple bitter rot and Glomerella leaf spot in China. *J. Fungi* **2022**, *8*, 740. [CrossRef]

73. Xu, M.; Zhou, Y.; Zhang, R.; Zeng, Y.-C.; Zhang, Y. First report of leaf spot caused by Colletotrichum siamense on Nageia nagi in China. In *Plant Disease*; The American Phytopathological Society (APS): St. Paul, MN, USA, 2022. [CrossRef]

74. Camiletti, B.X.; Lichtemberg, P.S.; Paredes, J.A.; Carraro, T.A.; Velascos, J.; Michailides, T.J. Characterization of Colletotrichum isolates causing Colletotrichum dieback of citrus in California. *Phytopathology®* **2022**, *112*, 1454–1466. [CrossRef]

75. Verma, R.; Das, A.; Chakrawarti, N.; Narzary, P.R.; Kaman, P.; Sharma, S. First report of black pepper (*Piper nigrum* L.) anthracnose caused by Colletotrichum siamense in north-east India. In *Plant Disease*; The American Phytopathological Society (APS): St. Paul, MN, USA, 2022. [CrossRef]

76. He, J.; Li, D.-W.; Bian, J.-Y.; Zhu, L.-H.; Huang, L. Unravelling species diversity and pathogenicity of Colletotrichum associated with anthracnose on Osmanthus fragrans in Quanjiao, China. *Plant Dis.* **2023**, *107*, 350–362. [CrossRef] [PubMed]

77. Huang, R.; Gui, Q.; Zhang, Y.; Sun, W.; Tang, L.; Huang, S.; Guo, T.; Li, Q.; Mo, J.; Huang, H. Identification and Observation of Infection Processes of Colletotrichum Species Associated with Pearl Plum Anthracnose in Guangxi, China. *Plant Dis.* **2022**, *106*, 3154–3165. [CrossRef] [PubMed]

78. Wang, X.; Liu, X.; Wang, R.; Fa, L.; Chen, L.; Xin, X.; Zhang, Y.; Tian, H.; Xia, M.; Hou, X. First report of Colletotrichum aenigma causing walnut anthracnose in China. *Plant Dis.* **2021**, *105*, 225. [CrossRef]

79. Zhang, Z.; Yan, M.; Li, W.; Guo, Y.; Liang, X. First Report of *Colletotrichum aenigma* Causing Apple Glomerella Leaf Spot on the Granny Smith Cultivar in China. *Plant Dis.* **2021**, *105*, 1563. [CrossRef]

80. Gunjan, S.; Marcel, M.; Meirav, E.; Stanley, F. First report of *Colletotrichum aenigma* and *C. perseae* causing anthracnose disease on Capsicum annuum in Israel. *Crop Prot.* **2022**, *152*, 105853. [CrossRef]

81. Hofer, K.M.; Braithwaite, M.; Braithwaite, L.J.; Sorensen, S.; Siebert, B.; Pather, V.; Goudie, L.; Williamson, L.; Alexander, B.J.; Toome-Heller, M. First report of Colletotrichum fructicola, *C. perseae*, and *C. siamense* causing anthracnose disease of avocado (*Persea americana*) in New Zealand. *Plant Dis.* **2021**, *105*, 1564. [CrossRef] [PubMed]

82. Alam, M.W.; Malik, A.; Rehman, A.; Hameed, A.; Tahir, U.; Sarwar, M.; Hussain, M.; Hussain, D.; Shafeeq, T. First record of Colletotrichum gloeosporioides causing anthracnose of banana in Pakistan. *Plant Dis.* **2021**, *105*, 2013. [CrossRef] [PubMed]

83. Slippers, B.; Stenlid, J.; Wingfield, M.J. Emerging pathogens: Fungal host jumps following anthropogenic introduction. *Trends Ecol. Evol.* **2005**, *20*, 420–421. [CrossRef] [PubMed]